RSC Advances

A systematic study of the variation of tetrathiafulvalene (TTF), TTF+• and TTF2+ reaction pathways with water in the presence and absence of light

Journal:	*RSC Advances*
Manuscript ID:	RA-ART-08-2014-008038.R1
Article Type:	Paper
Date Submitted by the Author:	12-Sep-2014

Complete List of Authors:	Adeel, Shaimaa; Monash University, Chemistry Li, Qi; Monash University, Chemistry Nafady, Ayman; Monash University, Chemistry Zhao, Chuan; Monash University, Chemistry Siriwardana, Amal; Monash University, Chemistry Bond, Alan; Monash University, Chemistry Martin, Lisandra; Monash University, Chemistry

A systematic study of the variation of tetrathiafulvalene (TTF), $TTF^{+\bullet}$ and TTF^{2+} reaction pathways with water in the presence and absence of light

Shaimaa M. Adeel,[a] Qi Li,[a] Ayman Nafady,[a,b] Chuan Zhao,[a,c] Amal I. Siriwardana,[a,d] Alan M. Bond*[a] and Lisandra L Martin*[a]

[a] School of Chemistry, Monash University, Clayton, Victoria 3800, Australia

* To whom correspondence should be addressed, Email: Lisa.Martin@monash.edu, Alan.Bond@monash.edu

[b] *Current Address:* King Saud University, College of Science, Department of Chemistry, PO Box 2455, Riyadh 11451, Saudi Arabia

[c] *Current Address:* School of Chemistry, The University of New South Wales, Sydney, NSW 2052, Australia

[d] *Current Address:* Tecnalia, Parque Tecnológico de San Sebastián, Mikeletegi Pasealekua, 2, E-20009 Donostia-San Sebastián, Gipuzkoa, Spain

Keywords: TTF, electrochemistry, photoreduction, water oxidation

Abstract

The chemistry of the strongly electron donating tetrathiafulvalene (TTF) molecule is exceptionally well known, but detailed knowledge of the chemistry of its technologically important one ($TTF^{+\bullet}$) and two (TTF^{2+}) electron oxidised redox partners is limited. In this paper, the different pathways that apply to the reaction of TTF, $TTF^{+\bullet}$, TTF^{2+} with water have been identified in the absence and presence of light. On the basis of data obtained by transient and steady state voltammetric methods in CH_3CN (0.1 M Bu_4NPF_6) containing 10% (v/v) H_2O, TTF is shown to participate in an acid base equilibrium reaction with $HTTF^+$, with H_2O acting as the proton donor. In contrast, $TTF^{+\bullet}$ generated by one electron bulk oxidative electrolysis of TTF remains unprotonated and fully stable in the presence of 10% H_2O in dark. However, when this cation radical is exposed to white or blue (λ = 425 nm) light, $TTF^{+\bullet}$ is photoreduced to TTF, with oxidation of water to give oxygen (detected by a Clark electrode) and protons that react with TTF to give $HTTF^+$ as the counter reaction. Again emphasising important reaction pathway differences associated with each redox level, TTF^{2+} generated by bulk two electron oxidative electrolysis of TTF reacts rapidly with water, even in the dark, to give $TTF^{+\bullet}$, protons, $HTTF^+$ and oxygen as the products.

1. Introduction

Tetrathiafulvalene (TTF) and its derivatives have attracted intense interest over a considerable time due to the strong electron donor ability as well as optical properties. These redox active molecules show a propensity to form strong H-bonds, π-stack to give stable radical dimers providing facile routes to novel molecular (and supramolecular) architectures, electrically conducting organic materials, stable charge-transfer compounds[1-7]. Some applications of derivatised TTF include functionalization with C_{60} creating self-assembled monolayers[8], quinoxaline for solar cells[9] and supramolecular assemblies[10] have been of enormous interest and it is therefore not surprising that TTF-derived materials have enabled a diverse range of technological applications, for example for nonlinear optics, sensors, and organic field-effect transistors[11-18]. So,

despite it being more than forty years[19] since the first semi-conducting, organic charge-transfer salt, TTF-TCNQ, (TCNQ = 7, 7, 8, 8-tetracyanoquinodimethane) was reported, there remains a paucity of detailed mechanistic data and knowledge on the underlying chemistries for the one and two electron oxidised $TTF^{+\bullet}$ and TTF^{2+} species.

Few studies have explored the chemistry of TTF with water, light and with oxygen. Noteably, Girault *et al.*[20] reported the four-electron reduction of oxygen to water by TTF chemistry using an acidified mixture of H_2O-dichloromethane solution. A report by Ndamanisha *et al.* in which a TTF-carbon composite was prepared to increase the electron donor ability of TTF was also found to reduce oxygen to water.[21] Clearly, as TTF is such a redox active molecule electrochemical techniques are invaluable tools to investigate the reactions of TTF, $TTF^{+\bullet}$ and TTF^{2+} especially with water, light and/or oxygen as reactants. In most organic solvents, TTF undergoes two well-separated, one-electron, chemically and electrochemically reversible oxidation processes, to generate the monocation radical, $TTF^{+\bullet}$ and with further oxidation, the dication (TTF^{2+})[2, 22-25] as described in equations 1 and 2;

$$TTF \rightleftharpoons TTF^{+\bullet} + e \qquad (1)$$

$$TTF^{+\bullet} \rightleftharpoons TTF^{2+} + e \qquad (2)$$

Thus, in acetonitrile, bulk oxidative electrolysis of TTF can quantitatively generate $TTF^{+\bullet}$ and TTF^{2+} and these products can be exposed to water and light in order to establish the reactivity of each redox level under relevant conditions. Acid-base chemistry of the TTF and its cations is also an important consideration. Giffard *et al.* [26] showed that TTF can be modified in acid media by protonation of the central C=C double bond[27-30] to give $HTTF^{+}$ (equation 3). This protonated species can also undergo reaction with another TTF molecule to give two TTF-based radicals, via a radical-substrate coupling, as described in equation 4.

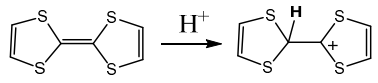

(3)

(4)

Here we provide a detailed investigation of the influence of water and light on $TTF^{0/+\bullet/2+}$ chemistry in the CH_3CN-H_2O (90:10) solvent mixture. In particular, reactions of TTF and the $TTF^{+\bullet}$ and TTF^{2+} cations, generated electrochemically, have been studied by voltammetric and spectroscopic techniques in CH_3CN (0.1 M Bu_4NPF_6) solution containing deliberately added water under dark conditions or when exposed to light. Reactions of interest that have been established include protonation of TTF by H_2O, photoreduction $TTF^{+\bullet}$ in the presence of H_2O, and evidence that TTF^{2+} is not stable under ambient conditions since it reacts with water to generate $TTF^{+\bullet}$ and $HTTF^{+}$.

2. Experimental Section

Materials and Chemicals. CH_3CN (HPLC grade, Merck) was distilled sequentially from calcium hydride, sodium metal in benzophenone and phosphorous pentoxide and stored in a glove box until required. TTF (99%, Aldrich), 54% ethereal HBF_4 (Aldrich), 2-propanol (BDH), chloroform and acetone were used as supplied by the manufacturer. Tetrabutyl ammonium hexafluorophosphate (Bu_4NPF_6, 98%) was purchased from Wako Pure Chemical Industries, Japan and was recrystallized from ethanol (95%) and vacuum dried prior to its use. Universal indicator paper with a pH range of 1.0 to 11.0 was purchased from Tokyo Roshi Kaisha, Japan.

Chemical Synthesis. (HTTF)BF_4 was synthesized as follows using a modified literature procedure.[26] TTF (2.5 mmol) was dissolved in 10 mL of anhydrous $CHCl_3$ under a nitrogen atmosphere. 40 mL of a 54 % ethereal HBF_4 (3.0 mmol) was dissolved in 10 mL of anhydrous $CHCl_3$ under and added slowly to the TTF solution at room temperature. This mixture was stirred

for 1hour after which the desired product was obtained as a dark-red powder. The crude solid was recrystallized from anhydrous CH_3CN at -20 °C which afforded fine dark red needles. The composition was confirmed to be (HTTF)BF_4 by ^{1}H NMR spectroscopy. [26]

Electrochemistry. Cyclic voltammetric measurements were undertaken at 22 ± 1 ^oC with a BAS100 electrochemical workstation interfaced to a standard three-electrode electrochemical cell configuration. Glassy carbon (GC) (3 mm or 1 mm diameter), gold (Au, 1 mm diameter), platinum (Pt, 1.6 mm), carbon fibre (C, 7 μm or 12 μm diameter) disks or indium tin oxide (ITO)-coated glass with an area of 0.06-0.1 cm^2 and 8-12 Ω sq^{-1} sheet resistance, obtained from Delta technologies, were used as the working electrodes. GC, Au and Pt electrodes were polished with 0.3 μm aqueous alumina slurries, rinsed with distilled water, acetone and then dried with nitrogen gas prior to each measurement. ITO electrodes were cleaned by sonication in acetone and then 2-propanol for 5 min prior to use. Ag/Ag^+ (10 mM $AgNO_3$ in CH_3CN, 0.1 M Bu_4NPF_6) was used as the reference electrode and platinum wire as the counter electrode. All solutions were degassed with the nitrogen gas saturated with the CH_3CN vapour for 10 min prior to commencing voltammetric measurements. 0.1 M Bu_4NPF_6 was used as the supporting electrolyte in neat CH_3CN or CH_3CN-H_2O mixtures.

Hydrodynamic voltammetric measurements with a rotating disk electrode (RDE) were performed with the BAS100 electrochemical workstation combined with a BAS MF-2066 glassy carbon rotating disk working electrode (A = 0.0707 cm^2) and the same reference and auxiliary electrodes as used for cyclic voltammetry. RDE measurements were performed in an electrochemical cell specially designed for small volumes.[31]

Bulk electrolysis experiments were used to generate the one- and two-electron oxidized species (TTF^+ and TTF^{2+}) in a three compartment cell, with each compartment being separated by a fine glass frit to minimize solution mixing. A large-area GC felt cloth (2 × 2 cm) (Tokai Carbon Japan) or a BAS GC basket net were used as working electrodes.

Unless others stated, potentials are referred to the ferrocene/ferrocenium ($Fc^{0/+}$) reference couple. Thus, the measured potential vs. Ag/Ag^+ was converted to the ferrocene scale via measurement of the reversible formal potential of the $Fc^{0/+}$ redox couple vs. Ag/Ag^+ under the relevant conditions. The potential of the Ag/Ag^+ reference electrode is -85 mv vs. $Fc^{0/+}$

Evolution of oxygen was detected using a Clark electrode (Unisense, Aarhus, Denmark). This membrane-based sensor was calibrated daily using the two-point method recommended by Unisense (0% and 100% air saturation). For photochemical experiments with oxygen concentration monitoring the solution was initially purged with nitrogen for 5 minutes to remove oxygen and then sealed to avoid the introduction of oxygen gas from the atmosphere.

In photochemical experiments, light from a Polilight PL6 (λ = 275–750 nm) Xe source (Rofin) was used. The total power output of the lamp at the end of the liquid light guide was 7 W. Full information about the light source are available in the manual.[32] In these experiments, the light source was positioned to one side of the soda glass vial at a distance of 10 cm from the wall-solution interface. Care was taken to avoid exposure of the Clark electrode to the light source. The photochemical reaction takes place with this configuration gives rise to a heterogeneous solution with maximum generation of products being achieved in the solution located near the cell wall.[31]

3. RESULTS AND DISCUSSION

Voltammetry of TTF in CH_3CN-H_2O mixtures

Cyclic voltammograms for the oxidation of 1 mM TTF in CH_3CN (0.1 M Bu_4NPF_6) in the absence and the presence of 10% H_2O are shown in Figure 1, obtained with a scan rate at 100 mV s^{-1} at a GC electrode. In the absence of H_2O, TTF exhibits two diffusion controlled, one-electron, reversible oxidation processes described by equations 1 and 2, as well documented in the literature. The midpoint potentials (E_m), calculated as the average of the oxidation $\left(E_p^{ox}\right)$ and reduction (E_p^{red1}) peak potential are -74 and 311 mV vs ferrocene ($Fc^{0/+}$) in CH_3CN and when 10% water is

present shift to -94 and 285 mV, respectively. E_m is approximately equal to the reversible formal potential E_f^0. The peak-to-peak separation (ΔE_p) for oxidation and reduction processes are about 80 mV for both oxidations at a scan rate of 100 mV s^{-1} and in both solutions. This value is higher than that theoretically predicted value of about 60 mV expected for a reversible process and implies that a small level of uncompensated ohmic drop (iR_u) is present, as also found for the well known reversible oxidation of Fc under the same conditions.[33] The oxidation peak potentials (E_p^{ox1}, E_p^{ox2}), reduction peak potentials (E_p^{red1}, E_p^{red2}) and midpoint potentials (E_{m1}, E_{m2}) in the absence and presence of 10% H_2O are summarized in Table S1. Addition of water to the CH_3CN solution shifts these potentials slightly to more negative values (*vs* Ag/Ag^+), probably due to the introduction of a liquid junction potential. A similar negative shift is observed for oxidation of ferrocene in the presence of H_2O (Figure S1). Interestingly, for TTF in the presence of 10% H_2O, although the electrochemical reversibility of the two oxidation processes is retained, an additional small irreversible oxidation reaction (E_p^{ox3} = 950 mV) is evident, lying at more positive potentials than for the $TTF^{+\bullet/2+}$ process (Figure 1). This new process is located at the same potential as found for oxidation of $HTTF^+$ (as discussed below), which implies that water acts as a proton donor to convert a small amount of TTF to $HTTF^+$ (equation 5) which is then oxidized as described in equations 6 and 7. Commonly, acid–base reactions are rapid and in equilibrium on the voltammetric time scale. However, in the present situation, the structures of TTF and $HTTF^+$ differ substantially (see the structures in equation 3),[26] so the acid-base chemistry is expected to be kinetically slow, allowing the observation of a separate oxidation processes when mixtures of both species are present. Since the cyclic voltammetric data at Au, Pt and ITO electrodes are similar to that at a GC electrode (Figure S2), surface interaction is not believed to be significant here, although changes in peak current are observed associated with variation of electrode area.

$$TTF + H_2O \rightleftharpoons HTTF^+ + OH^- \quad (5)$$

$$HTTF^+ \rightleftharpoons HTTF^{2+} + e \quad (6)$$

$$HTTF^{2+} \rightleftharpoons Product(s) \quad (7)$$

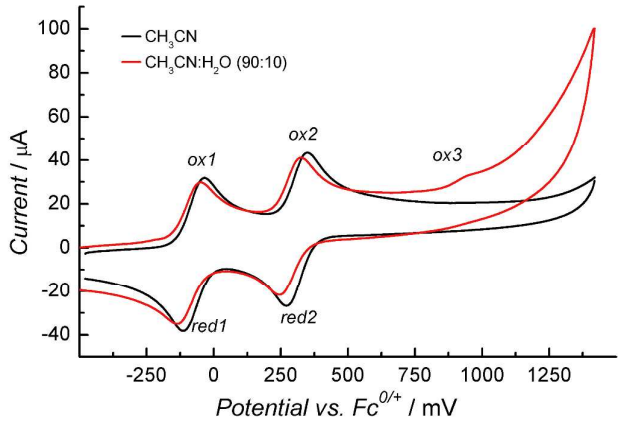

Figure 1 Cyclic voltammograms for the oxidation of 1 mM TTF in CH_3CN (0.1 M Bu_4NPF_6) obtained with a 3 mm diameter GC electrode using a scan rate of 100 mV s^{-1} in the absence and presence of 10 % H_2O.

Steady-state voltammograms obtained with a carbon fiber microelectrode (12 *μ*m diameter) in the absence and in the presence of 10% H_2O (Figure S3) confirms that the two TTF oxidation processes are electrochemically reversible, as differences in the potentials ($E_{3/4}-E_{1/4}$) are 60 mV. Thus the half-wave potentials ($E_{1/2}$) are almost identical to the mid-potentials (E_m) obtained from cyclic voltammograms at a 3 mm diameter GC electrode. Diffusion coefficients of TTF in CH_3CN in the absence and in the presence of 10% H_2O were calculated using these steady state voltammograms and are 2.1 x 10^{-5} and 2.0 x 10^{-5} cm^2 s^{-1}, respectively. These values are also in excellent agreement those derived from the transient voltammetry using the Randles-Sevcik equation [33] of 2.2 x 10^{-5} (absence of water) and 2.1 x 10^{-5} cm^2 s^{-1} (10% water present) and also with the value of D_{TTF} of 2.2 x 10^{-5} cm^2 s^{-1} reported by Norton *et al.* in CH_3CN.[34]

Photochemical oxidation of H_2O by $TTF^{+\bullet}$

In the absence of water, both $TTF^{+\bullet}$ and TTF^{2+} can be quantitatively produced by oxidative bulk electrolysis of neutral TTF (1 mM) in CH_3CN (0.1 M Bu_4NPF_6) using an applied potential (E_{appl}) of 120 mV and 620 mV (vs. $Fc^{0/+}$) respectively.[35] This outcome is confirmed by noting the change in the relative position of the zero current in the GC rotating disk electrode (RDE) voltammograms before and after stepwise bulk electrolysis to generate a persistent solution of the red coloured $TTF^{+\bullet}$ or the yellow coloured TTF^{2+} (Figure S4).

In the presence of 10% H_2O, in the dark (Figure S3), the time independent zero current position and limiting current magnitude confirmed the stability of $TTF^{+\bullet}$. However, cyclic voltammograms for a 1 mM $TTF^{+\bullet}$ solution in CH_3CN containing 10% H_2O (0.1 M NBu_4PF_6) change after exposure to light (Figure 2). Irradiation with white light from a Xe source (λ = 275-750 nm) for 2 min, resulted in an irreversible oxidation process appearing at about 950 mV, which is assigned to the oxidation of $HTTF^+$. Furthermore, after 10 minutes irradiation, the apparent "pH" of the solution (determined using pH paper) dropped to ~3-4 indicating that the solution became acidic. The voltammetric parameters for the $TTF^{+\bullet}$ redox processes, in the presence and absence of H_2O and/or light are summarized in Table S2.

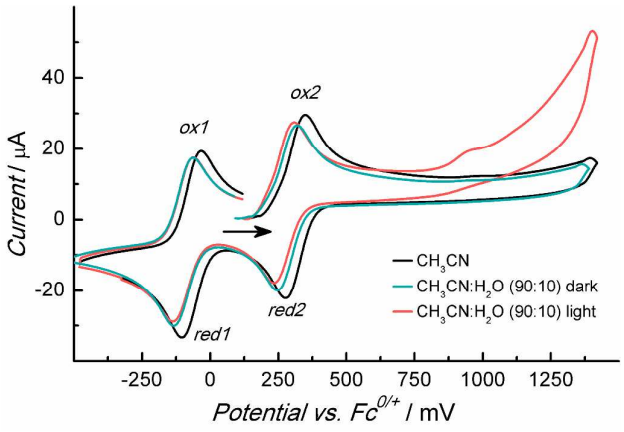

Figure 2 Cyclic voltammograms obtained with a 3 mm diameter GC electrode at a scan rate of 100 mV s^{-1} showing the ($TTF^{+\bullet/2+}$) oxidation and ($TTF^{+\bullet/0}$) reduction processes derived from 1mM $TTF^{+\bullet}$ solutions in CH_3CN and mixed CH_3CN/H_2O (90:10%) solvent media (0.1 M Bu_4NPF_6) in the dark and after irradiation with white light (λ = 275-750 nm) for 2 min.

The UV-visible spectrum of the red coloured, electrochemically generated $TTF^{+\bullet}$ solution in CH_3CN (0.1 M Bu_4NPF_6) is shown in Figure S5. Absorption maxima are observed at wavelengths (λ_{max}) of 355 nm and 273 nm for TTF^{2+}, at 335, 430 and 579 nm for $TTF^{+\bullet}$, while TTF exhibits two absorption bands with λ_{max} at 302 and 317 nm. These spectra are also in good agreement with those reported in the literature[6, 36, 37].

Irradiation of the $TTF^{+\bullet}$ solution in neat CH_3CN using white light for 10 min, had no effect on the UV-visible spectrum, implying $TTF^{+\bullet}$ is stable in dry CH_3CN in the presence of light. However, in the presence of water $TTF^{+\bullet}$ is photochemically unstable as shown in Figure 2 and 3. Figure 3 shows the steady state voltammograms resulting from a $TTF^{+\bullet}$ solution in CH_3CN with 10% H_2O before and after exposure to white light. In the dark, the relative position of the zero current remains unchanged and similar to that obtain in neat CH_3CN, confirming that $TTF^{+\bullet}$ is stable in the presence of 10% H_2O. However, upon exposure to white light, the relative position of zero current shifts to a value that reveals the solution now contains TTF as well as $TTF^{+\bullet}$. Increasing the irradiation time, the concentration of $TTF^{+\bullet}$ present in the solution decreases to a negligible value while TTF and $HTTF^{+}$ increases, concomitantly. Thus, this observation indicates that $TTF^{+\bullet}$ is photoreduced in the presence of H_2O, which also implies that H_2O is oxidized in the counter redox reaction. A reaction scheme for this photoactivity is proposed in equations 8-10. If this scenario is correct, in the presence of light, $TTF^{+\bullet}$ can oxidize H_2O directly to oxygen.

$$4\,TTF^{+\bullet} \xrightarrow{hv} 4\,(TTF^{+\bullet})^{*} \qquad (8)$$

$$4\,(TTF^{+\bullet})^{*} + \; 2\,H_2O \;\longrightarrow\; 4\,TTF \;+\; O_2 \;+\; 4\,H^{+} \qquad (9)$$

$$4\,TTF \;+\; 4\,H^{+} \;\longrightarrow\; 4\,HTTF^{+} \qquad (10)$$

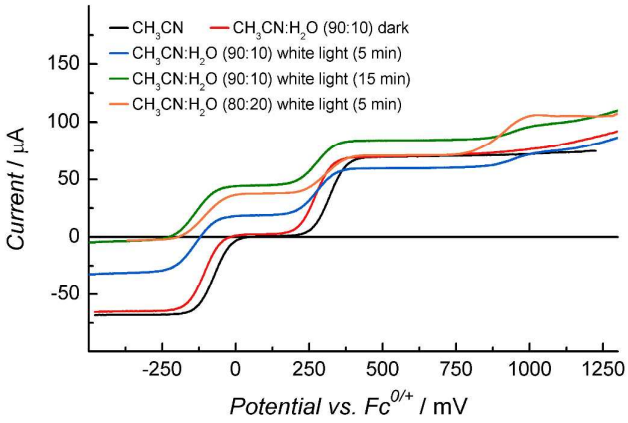

Figure 3 Voltammograms for 1 mM $TTF^{+\bullet}$ (obtained by bulk electrolysis) in CH_3CN and in (90:10) (v/v) CH_3CN:H_2O (0.1 M Bu_4NPF_6) before and after irradiation with white light for designated periods of time. These data were obtained with a 3 mm diameter GC RDE (rotation rate 1000 rpm).

To confirm that oxygen is a product of irradiation of CH_3CN $TTF^{+\bullet}$ solutions that contained H_2O a Clark electrode was used. The experiment required removal of adventisious oxygen by rigorous degassing with nitrogen and the reaction cell was tightly sealed to ensure that no atmospheric oxygen could be introduced. The data obtained using the Clark electrode (Figure 4), shows the oxygen percentage relative to the solubility limit, as a function of irradiation time for a 1 mM $TTF^{+\bullet}$ in neat CH_3CN solution and with water present. In the absence of H_2O, the oxygen concentration remains close to zero even when the 1 mM $TTF^{+\bullet}$ solution is illuminated with white light (275-750 nm). Similarly, no oxygen is detected or change in the intensity of the red coloured $TTF^{+\bullet}$ solution observed, with or without 10% H_2O, in the dark. In contrast, with H_2O present and under irradiation with white light, an increase in oxygen concentration was clearly detected and the solution colour changed from red to yellow. Together these outcomes are all consistent with photo-reduction of

$TTF^{+\bullet}$ to the neutral TTF and the photo-oxidation of H_2O to O_2. This photochemical irradiation of $TTF^{+\bullet}$ was repeated using 425 nm visible light, which lies close to the value of λ_{max} 430 nm for the TTF mono cation. Under these conditions, evolution of oxygen was still detected, but the rate of increase was less than that with white light. Additionally, it was found that the rate of oxygen generation is enhanced in the presence of 20% H_2O relative to that found with 10% H_2O. In summary the irradiation $TTF^{+\bullet}$ detects the evolution of oxygen and a change in solution colour in the presence of aqueous CH_3CN and together with the voltammetric data are consistent with the reaction scheme summarized in equations 8-10.

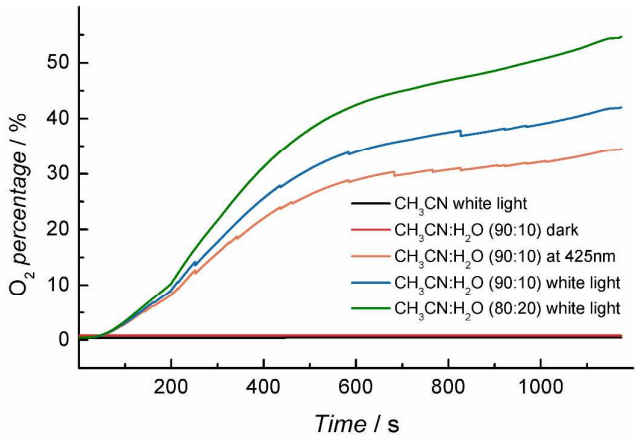

Figure 4 Oxygen percentage as a function of time for 1 mM $TTF^{+\bullet}$ in CH_3CN (0.1 M Bu_4NPF_6) with or without added H_2O in the dark, under exposure to irradiation with white light (at 275-750 nm) or 425 nm visible light.

Instability of TTF^{2+} in the presence of water

As described above, $TTF^{+\bullet}$ reacts with water when exposed to light to give TTF and O_2. In contrast, the dication TTF^{2+} reacts with H_2O rapidly, even in the dark, as briefly noted in a paper Siedle *et al.*[38] In order to explore this process in more detail, TTF^{2+} was quantitatively generated by exhaustive oxidization of a 1 mM TTF in CH_3CN (0.1 M Bu_4NPF_6) at 620 mV (vs. $Fc^{0/+}$) in a carefully sealed electrochemical cell placed in a dry box to avoid the introduction of water. During this bulk electrolysis experiment, the initial light-yellow TTF solution changed colour initially to the dark red ($TTF^{+\bullet}$) and then to a light yellow (TTF^{2+}) solution. Steady state voltammetry of the TTF^{2+} solution was undertaken 10 minutes after the bulk electrolysis, at a GC electrode. The position of zero current confirmed that complete oxidation of TTF to TTF^{2+} was achieved (Figure 5). The solution was taken from the anaerobic conditions and cyclic voltammetry detected an additional oxidation process at ~ 950 mV (Figure S6) increased with time over a few minutes together with a change of the solution colour from light yellow to orange after ~20 minutes. Addition of 10% (v/v) H_2O to the CH_3CN solution containing 1 mM TTF^{2+}, resulted in the light yellow solution immediately turn dark purple-red, the colour expected for a $TTF^{+\bullet}$ solution. The apparent "pH" of this solution was checked after 5 minutes (using of pH paper), indicating a value of ~3, hence the solution is now acidic. A control experiment with no TTF^{2+} present and containing 10% H_2O (v/v) in CH_3CN (0.1 M Bu_4NPF_6) showed the apparent "pH" value remained in the 6-7 range. Thus, the instability of TTF^{2+} in presence of H_2O generates protons.

The new oxidation process found in the transient and steady state voltammograms of TTF^{2+} at ~ 950 mV (Figure 5 and S6) are consistent with the reaction between TTF^{2+} and H_2O generating protonated $HTTF^{+}$ species. The steady state voltammetric conditions show the current for the $TTF^{2+/+\bullet}$ and $TTF^{+\bullet/0}$ reduction processes decrease to a very small level. Using the position of zero current as a starting point, the residual material is $TTF^{+\bullet}$ (~20%) and nearly 80% of the TTF^{2+} has been converted to $HTTF^{+}$ (equation 11).

$$2\ TTF^{2+} + \ 2\ H_2O \ \longrightarrow \ 2\ HTTF^{+} \ + \ O_2 \ + \ 2\ H^{+} \qquad (11)$$

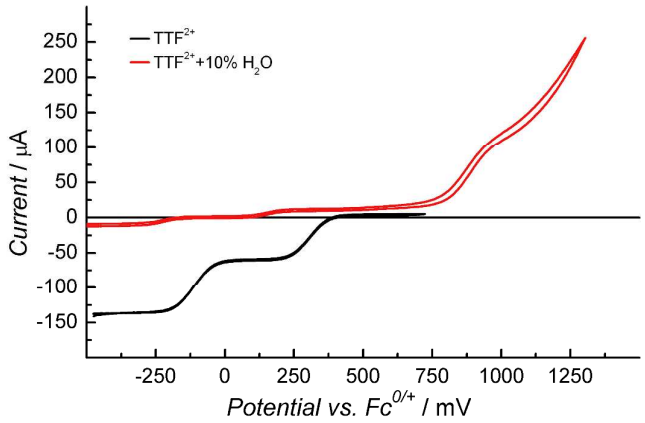

Figure 5 Steady state voltammograms for 1mM TTF^{2+} generated by bulk electrolysis in CH_3CN (0.1 M Bu_4NPF_6) in the absence and in the presence of 10% H_2O obtained at a 3 mm GC electrode.

Once again using a sealed reaction cell, a Clark electrode was used to confirm oxygen evolution from TTF^{2+} solutions in which water was present. The data in Figure S7 show no oxygen evolution for TTF^{2+} in neat CH_3CN compared with significant oxygen evolution for 1 mM TTF^{2+} CH_3CN solution after dilution of 10% H_2O, under a nitrogen atmosphere and exposed to light. The colour of the TTF^{2+} solution was also observed to change from yellow to red in the presence of water, also consistent with formation of $HTTF^{+}$.

Electrochemical characterization of $HTTF^{+}$

Previous studies by Giffard *et al.*[16] noted that $HTTF^{+}$ reverted back to neutral TTF once dissolved in aqueous media, but they did not provide any mechanistic details. Using $(HTTF)BF_4$ we undertook voltammetric studies to obtain a more detailed understanding of the reactions of TTF, $TTF^{+\bullet}$ and TTF^{2+} with H_2O in the dark and on irradiation with light.

Cyclic voltammograms for $(HTTF)BF_4$ in CH_3CN (0.1 M Bu_4NPF_6) are shown in Figure 6. In addition to both the $TTF^{0/+\bullet}$ and $TTF^{+\bullet/2+}$ reversible redox processes are present, an irreversible oxidation process at 950 mV is well defined. There are characteristics similar to the voltammagram in Figure 1 following the addition of 10% H_2O to the CH_3CN solution. The presence of the reversible redox processes for $TTF^{0/+\bullet}$ and $TTF^{+\bullet/2+}$ following dissolution of $(HTTF)BF_4$ in CH_3CN suggests that an equilibrium reaction, in equation 12, occurs.

$$HTTF^+ \rightleftharpoons TTF + H^+ \qquad (12)$$

Therefore the irreversible oxidation process at 950 mV is due to the formation of $HTTF^{2+}$.

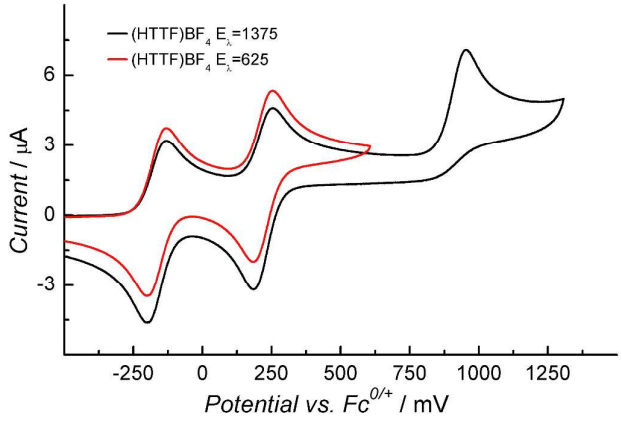

Figure 6 Cyclic voltammograms for 1 mM $(HTTF)BF_4$ in CH_3CN (0.1 M Bu_4NPF_6) using a scan rate of 100 mV s^{-1} at designated switching potentials (E_λ) obtained with a 3 mm diameter GC electrode. Cyclic voltammograms were obtained under rigorous dry, anerobic conditions.

4. Conclusions

We have systematically examined the voltammetric behaviour of TTF, $TTF^{+\bullet}$, TTF^{2+} and $HTTF^+$ in CH_3CN (0.1 M Bu_4NPF_6) in the presence of water and light in order to elucidate the relationship between their chemistries and photochemistry under ambient condition. This has resulted in

identification of several different pathways for the reaction of TTF and its cations in water with or without light. TTF reacts with H_2O to form $HTTF^+$. $TTF^{+\bullet}$ reacts with water to give TTF, $HTTF^+$ and O_2, under irradiation with light. Mechanistically, $TTF^{+\bullet}$ is photo-reduced to TTF and H_2O is oxidized to oxygen, releasing protons in these photochemical reactions. Monitoring the irradiated $TTF^{+\bullet}$ solution with a Clark electrode confirms the evolution of oxygen in CH_3CN solution containing 10% H_2O. Confirmation of the instability of TTF^{2+} under ambient conditions revealed that the TTF^{2+} dication reacts with H_2O to generate $TTF^{+\bullet}$ and $HTTF^+$. Together, the photochemistry and the voltammetric measurements reveal important reaction pathway differences for TTF, $TTF^{+\bullet}$, TTF^{2+} and $HTTF^+$ redox chemistries in the presence of H_2O and light. Knowledge of the chemistry under ambient conditions should assist the development of practical devices derived from use of TTF based materials.

Acknowledgments

AMB and LLM gratefully acknowledge financial support from the Australian Research Council. SA gratefully acknowledges receipt a Monash Graduate Scholarship and we thank Mr Muhammad Abdelhamid for his assistance with the Figures.

References

1. J. L. Segura and N. Martín, *Angew. Chem. Int. Ed.*, 2001, **40**, 1372-1409.
2. F. Wudl, G. M. Smith and E. J. Hufnagel, *J. Chem. Soc. D, Chem. Commun.*, 1970, 1453-1454.
3. Y. Wang, S. Cui, B. Li, J. Zhang and Y. Zhang, *Crystal Growth & Design*, 2009, **9**, 3855-3858.
4. E. Coronado, Giménez-Saiz, Carlos Gómez-García and C. J., *Coord. Chem. Rev.*, 2005, **249**, 1776-1796.
5. E. Coronado, J. R. GalanMascaros, C. GimenezSaiz, C. J. GomezGarcia and V. N. Laukhin, *Adv. Mater.*, 1996, **8**, 801-803.
6. R. Andreu, J. Garín and J. Orduna, *Tetrahedron*, 2001, **57**, 7883-7892.
7. N. Dupont, Y.-F. Ran, S.-X. Liu, J. Grilj, E. Vauthey, S. Decurtins and A. Hauser, *Inorg. Chem.*, 2012, **52**, 306-312.
8. C. M. Davis, J. M. Lim, K. R. Larsen, D. S. Kim, Y. M. Sung, D. M. Lyons, V. M. Lynch, K. A. Nielsen, J. O. Jeppesen, D. Kim, J. S. Park and J. L. Sessler, *J. Am. Chem. Soc.*, 2014, **136**, 10410-10417.
9. A. Amacher, C. Yi, J. Yang, M. P. Bircher, Y. Fu, M. Cascella, M. Gratzel, S. Decurtins and S.-X. Liu, *Chem. Commun.*, 2014, **50**, 6540-6542.
10. M. Frasconi, T. Kikuchi, D. Cao, Y. Wu, W.-G. Liu, S. M. Dyar, G. Barin, A. A. Sarjeant, C. L. Stern, R. Carmieli, C. Wang, M. R. Wasielewski, W. A. Goddard and J. F. Stoddart, *J. Am. Chem. Soc.*, 2014.
11. M. R. Bryce, *J. Mater. Chem.*, 2000, **10**, 589-598.
12. J. Bigot, B. Charleux, G. Cooke, F. o. Delattre, D. Fournier, J. l. Lyskawa, L. n. Sambe, F. o. Stoffelbach and P. Woisel, *J. Am. Chem. Soc.*, 2010, **132**, 10796-10801.
13. W. Sun, C.-H. Xu, Z. Zhu, C.-J. Fang and C.-H. Yan, *J. Phys. Chem.*, 2008, **112**, 16973-16983.
14. M. D. Halling, J. D. Bell, R. J. Pugmire, D. M. Grant and J. S. Miller, *J. Phys. Chem. A*, 2010, **114**, 6622-6629.
15. D. M. Guldi, L. Sánchez and N. Martín, *J. Phys. Chem. B*, 2001, **105**, 7139-7144.
16. T. Akutagawa, K. Kakiuchi, T. Hasegawa, S.-i. Noro, T. Nakamura, H. Hasegawa, S. Mashiko and J. Becher, *Angew. Chem. Int. Ed.*, 2005, **44**, 7283-7287.
17. J. M. Williams, A. J. Schultz, U. R. S. Geiser, K. D. Carlson, A. M. Kini, H. H. Wang, W.-K. Kwok, M.-H. Whangbo and J. E. Schirber, *Science*, 1991, **252**, 1501-1508.
18. Z. Yu, H. Tian, E. Gabrielsson, G. Boschloo, M. Gorlov, L. Sun and L. Kloo, *RSC Advances*, 2012.
19. J. Ferraris, D. O. Cowan, V. Walatka and J. H. Perlstein, *J. Am. Chem. Soc.*, 1973, **95**, 948-949.

20. A. J. Olaya, P. Ge, J. r. m. F. Gonthier, P. Pechy, C. m. Corminboeuf and H. H. Girault, *J. Am. Chem. Soc.*, 2011, **133**, 12115-12123.

21. J. C. Ndamanisha, X. Bo and L. Guo, *Analyst*, 2010, **135**, 621-629.

22. J. M. Spruell, A. Coskun, D. C. Friedman, R. S. Forgan, A. A. Sarjeant, A. Trabolsi, A. C. Fahrenbach, G. Barin, W. F. Paxton, S. K. Dey, M. A. Olson, D. Benítez, E. Tkatchouk, M. T. Colvin, R. Carmielli, S. T. Caldwell, G. M. Rosair, S. G. Hewage, F. Duclairoir, J. L. Seymour, A. M. Z. Slawin, W. A. Goddard, M. R. Wasielewski, G. Cooke and J. F. Stoddart, *Nat Chem*, 2010, **2**, 870-879.

23. A. Y. Ziganshina, Y. H. Ko, W. S. Jeon and K. Kim, *Chem. Commun.*, 2004, 806-807.

24. Q. Li, C. Zhao, A. M. Bond, J. F. Boas, A. G. Wedd, B. Moubaraki and K. S. Murray, *J. Mater. Chem.*, 2011, **21**, 5398-5407.

25. S. J. Shaw, F. Marken and A. M. Bond, *Electroanalysis*, 1996, **8**, 732-741.

26. M. Giffard, P. Frere, A. Gorgues, A. Riou, J. Roncali and L. Toupet, *J. Chem. Soc., Chem. Commun.*, 1993, 944-945.

27. Y. Kobayashi, M. Yoshioka, K. Saigo, D. Hashizume and T. Ogura, *J. Am. Chem. Soc.*, 2009, **131**, 9995-10002.

28. M. Giffard, M. Sigalov, V. Khodorkovsky, A. Gorgues and G. Mabon, *Synth. Met.*, 1999, **102**, 1713-1713.

29. M. Giffard, A. Gorgues, A. Riou, J. Roncali, T. P. Nguyen, J. Garín, S. Uriel and P. Alonso, *Synth. Met.*, 1995, **70**, 1133-1134.

30. M. Giffard, P. Alonso, J. Garin, A. Gorgues, T. P. Nguyen, P. Richomme, A. Robert, J. Roncali and S. Uriel, *Adv. Mater.*, 1994, **6**, 298-300.

31. G. Bernardini, C. Zhao, A. G. Wedd and A. M. Bond, *Inorg. Chem.*, 2011, **50**, 5899-5909.

32. Rofin Polilight PL6 manual, http://www.rofin.com.au.

33. A. M. Bond, *Broadening Electrochemical Horizons: Principles and Illustration of Voltammetric and Related Techniques*, Oxford University Press, 2002.

34. J. D. Norton, W. E. Benson, H. S. White, B. D. Pendley and H. D. Abruna, *Anal. Chem.*, 1991, **63**, 1909-1914.

35. A. M. Bond, K. Bano, S. Adeel, L. L. Martin and J. Zhang, *ChemElectroChem*, 2013, 1 (1) 99-107.

36. L. Huchet, S. Akoudad, E. Levillain, J. Roncali, A. Emge and P. Bäuerle, *J. Phys. Chem. B*, 1998, **102**, 7776-7781.

37. J.-F. Bergamini, P. Hapiot and D. Lorcy, *J. Electroanal. Chem.*, 2006, **593**, 87-98.

38. A. R. Siedle, G. A. Candela, T. F. Finnegan, R. P. Van Duyne, T. Cape, G. F. Kokoszka, P. M. Woyciejes and J. A. Hashmall, *Inorg. Chem.*, 1981, **20**, 2635-2640.

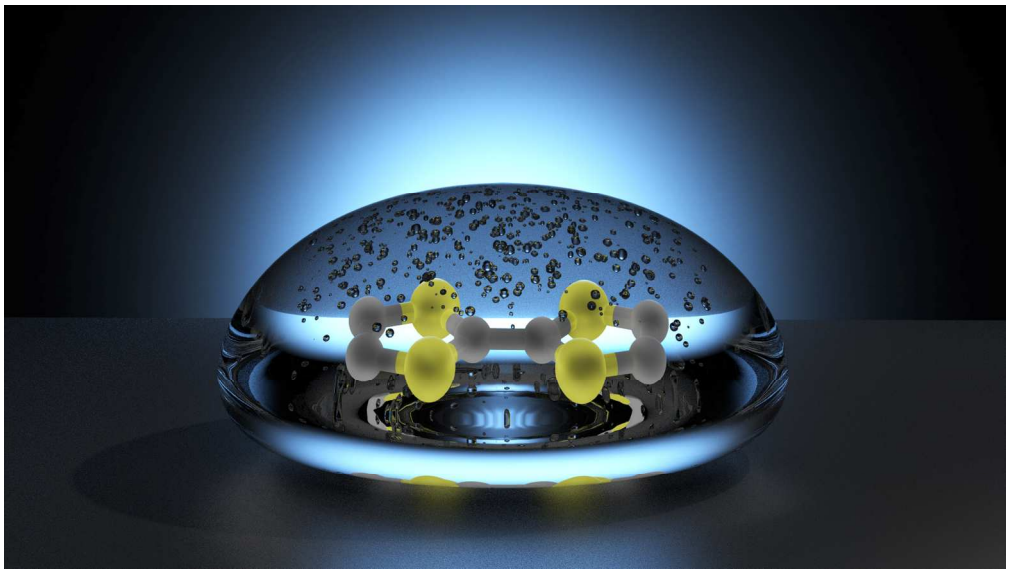

The chemistry of TTF0/+/2+ and HTTF+ in acetonitrile/water uses different reaction pathways eg. illumination of TTF+ oxidises water to O2.
677x381mm (72 x 72 DPI)

Table of Content entry

The chemistry of $TTF^{0/+/2+}$ and $HTTF^{+}$ in acetonitrile/water uses different reaction pathways *eg.* illumination of TTF^{+} oxidises water to O_2.